



Preparation of Polyamide-6/zeolite-Y Hybrid Membranes, and the evaluation of their Structural, Physical and Mechanical Properties

*Oula Adnan Hommaid, and Iman Mostafa Al Bakri

Department of Chemistry, Faculty of Science, Damascus University, Syrian Arab Republic



Abstract

A well-defined crystalline structure of zeolite-Y, having particles size in the range from 100 to 270nm, was prepared using hydrothermal method. The obtained zeolite was further used to fabricate polyamide-6/zeolite-Y (PA6/ZY) hybrid membranes. The addition of ZY modified the smooth surface of PA6 membrane, and the Scanning Electron Microscopy (SEM) images of PA6/ZY became rough with increasing porosity. X-ray diffraction (XRD) revealed an exfoliated structure of the hybrid membranes. Moreover, Fourier transforms infrared spectroscopy (FTIR) of PA6/ZY membranes indicated the presence of some interaction between the PA6 and ZY, which was manifested itself by the slight increase in the intensity of PA6 bands after the addition of ZY.

The results indicated that the tensile strength and failure strain decreased linearly with the increase of ZY content in the hybrid membranes. On the other hand, porosity and bubble point pore diameter increased gradually and reached a maximum when 4% ZY was added. It was concluded that 4%w loading of ZY in the hybrid membranes gave a balance of desirable properties and the hybrid membrane could be considered promising for water separation technology.

Key words: Zeolite -Y, polyamide-6, hybrid membrane, physical and mechanical properties.

Introduction

Membranes have gained an important position in chemical technology, and they have been used in a broad range of applications. The key property of membranes is their ability to control the permeation rate of a chemical species through them [1]. A microporous membrane is very similar in structure and function to the conventional filter. It has rigid, highly voided structure with randomly distributed, interconnected pores [1,2]. Synthetic membranes have been fabricated from a wide variety of organic (e.g. polymer) or inorganic (e.g. zeolites) materials since early 1960s. However, hybrid membranes that utilize both inorganic and organic materials are still less common [3]. The most widely used synthetic polymers in membranes are polyamide-6 (PA-6), polyamide-66 (PA-66), polysulfone (PS), polyethersulfone (PES), polyvinylidene difluoride (PVDF) and polypropylene (PP) because they have

good chemical, thermal and mechanical stabilities [4].

Among them, polyamide-6 has an excellent combination of desirable properties, including hydrogen bond in molecular chains [5], fatigue resistance, high tensile strength, abrasion and good toughness [6]. These properties make it one of the major engineering and high performance plastic [5], and a good choice in the preparation of the hybrid membranes [7,8,9]. Addition of inorganic nanoparticles (clay) considerably improves the filtration of membrane by controlling the formation and growth of macrovoids [6]. It also increases the number of small pores and as a result improves hydrophilicity, porosity, permeability, mechanical and antifouling properties [6]. Different types of nanomaterials have been investigated for such applications including zeolite, silica, carbon nanotubes, mesoporous carbon, pure metals and

*Corresponding author e-mail: OULA-85@hotmail.com

Receive Date: 27 October 2019, Revise Date: 09 December 2019, Accept Date: 01 April 2020

DOI: 10.21608/EJCHEM.2019.18717.2155

©2020 National Information and Documentation Center (NIDOC)

nanometal oxides [10]. Among various nano particles, zeolite nano particles are now the most frequently used [10]. Recently, multi-layer polyamide-6 nanofibrous membranes were prepared by electrospinning and hot pressing methods for dye filtration [11]. In addition, Electrospun PA6 nanofiber hybrid membranes with superior performance were made and used in reverse osmosis [12]. Our work was directed to prepare PA/ZY hybride membranes utilizing hydrothermal method under the influence of self- pressure at 120°C and the immersion precipitation method. The resultant hybrid membranes were characterized using XRD, FTIR, and SEM. In addition, their characteristic as filtration and/or reverse osmosis membranes were evaluated by measuring the physical and mechanical properties. The prepared hybrid membrane will serve as the heart of a future practical device for water purification.

Materials and Methods

Materials and sample preparation:

Silica (Silica gel DG for thin- layer chromatography, Riedel-Dehaenvag Seelze- Hannover) , Polyamide-6 for column chromatography (Sigma-Aldrich), Sodium aluminate NaAlO_2 (Al(as Al_2O_3):50-54%,Na(as Na_2O):40-45%, Sigma-Aldrich), Sodium hydroxide (>99% w/w NaOH, Panrace), Formic acid ($d=1.22 \text{ g/cm}^3$, Purity 98%, Merck), Sodium metabisulfite solution (sham-lab) were used without any modifications. All solutions were prepared using distilled water. Zeolite-Y was prepared according to the method described by Karami *et al* [13] with some modification. NaOH (0.2g) and NaAlO_2 (0.145g) were added to 2 mL of water using the reactor shown in Figure 1. The mixture was stirred until a clear solution was obtained. The resulting solution was added to 0.5g of silica in a 40 mL Teflon bottle and stirred for 2 h, then left for 48-120 h for aging. The bottle was heated to 120 °C in an oven for 48 h under the influence of self-pressure, then it was cooled to room temperature before opening the reactor cover. The product was suspended in water and filtered by vacuum. The final product was dried at 100°C for 2 h. Immersion precipitation method was applied to prepare the membrane. A (22 % w) of polyamide-6 and (0-6) % w of zeolite were dissolved in 72–78 % w of formic acid with continuous stirring by a high speed homogenizer for 10 min. Then continue stirring using magnetic stirrer for a 24h, which

insured complete admixture. The solution was spread on a glass plate with a glass stick. The solvent was left to evaporate partially from the casting solution until the membrane becomes white in color, then the glass plate was immersed in a precipitation bath containing formic acid (10%) [6]. After precipitation, the membrane was removed and washed with distilled water. The membrane underwent thermal treatment by placing them in a water bath at 100 °C for one hour [4], then stored in sodium metabisulfite solution ($\text{Na}_2\text{S}_2\text{O}_5$ 1%) in a cool and dark place until used[14].



Instrumentation:

Elemental Analysis for zeolite, FTIR, XRD and SEM were used to determine the chemical composition of zeolite Y and the prepared membranes. Tensile test machine (K&H, Syria), Grinder (NU-5999 , Korea), Digital balance (Pricesa 240 A, Switzerland), Electronic Digital Caliper (N 610676, Austria), Reactor(K&H, Syria) were used. FTIR (JASCO FT-IR-4200, Japan), Xray diffraction (STOE STADI P, Germany) and SEM analysis (UEG Iixmu, Czechia) were provided by Atomic Energy Commission of Syria.

Characterization:

Membrane porosity

The membrane porosity (ϵ) is defined as the pores volume divided by the total volume of the porous membrane. It was calculated using (Equation (1)) [8].

$$\varepsilon = \frac{(m_0 - m_3)}{m_1 - (m_2 - m_0)} \times 100 \quad (1)$$

Where: m_3 is the dry membrane weight, m_0 is the wet membrane weight, m_1 is the weight of pycnometer full of water and m_2 is the weight of pycnometer after putting wet membrane into the full pycnometer. Measurements were repeated 3 times.

Pore size:

The bubble pressure test is based on measurements over come the pressure necessary to blow air through a water-filled porous membrane, where the pressure is enough to over come the surface tension of the liquide in the largest pore, where liquid is then rejected from the pore [15]. The equilibrium condition can be expressed in the Washburn equation presented in equation (2) [16]:

$$\Delta p = \frac{4\gamma \cos \theta}{D} \quad (2)$$

Where: D is equivalent diameter, γ is surface tension (N/m). θ is contact angle (water/air), where $\theta \approx 0$ ($\cos \theta=1$), and ΔP is pressure difference across the membrane given in (pa). All measurements were repeated three times and calculating the average.

Mechanical properties of membrane:

The tensile strength (σ) given in (pa) is the ratio of tensile load (F) at break applied on the specimen to its original cross-sectional area (A_0), before any load was applied, as in equation (3) [17]:

$$\sigma_b = \frac{F}{A_0} \quad (3)$$

Where: F is the force required to pull the specimen apart (N), and A_0 is specimen area (cm^2) $A_0 = b$ specimen width (cm) \times δ specimen thickness (cm). The specimen width is b (=0.8 cm), the specimen thickness is δ (=0.23cm).

Failure strain (ε) is a ratio of increase of specimen gauge length ΔL at rupture to its original gauge length L_0 as in equation (4) [17]:

$$\varepsilon_b = \frac{L - L_0}{L_0} = \frac{\Delta L}{L_0} \quad (4)$$

Where: L_0 (=1.2 cm) is the original length before any load applied, and L is instantaneous length (cm). Figure 2 represents the sample dimension used to measure the mechanical properties.

All measurements were repeated three times and the average was taken for all results.



Fig. 2. Standard tensile test specimen

Results and Discussion

Elemental Analysis:

Quantitative determinations of major elements in the zeolite were carried out with classical gravimetric method after complete dissolution of the sample. Table 3.1 shows the resulted percentage of Na_2O , Al_2O_3 , SiO_2 and H_2O in prepared zeolite sample.

Table 3.1 : Percentage of major compounds in the prepared zeolite

Elements	%
Na_2O	14.36
Al_2O_3	16.12
SiO_2	49.76
H_2O	19.76
Ratio ($\text{SiO}_2/\text{Al}_2\text{O}_3$)	3.09

The results (in the table (3.1)) indicated that the ratio $\text{SiO}_2/\text{Al}_2\text{O}_3$ is 3.09, which is in the range from 2 to 6, conforming that the prepared zeolite was of type Y [18,19,20].

FTIR Spectroscopic Analysis:

The FTIR spectrum of the crystalline structure of prepared zeolite Y is shown in Figure 3. The peak around 1600 cm^{-1} refers to bending vibration of adsorbed water molecule and the band in the range $3365\text{-}3489 \text{ cm}^{-1}$ is assigned to OH stretching [20]. The band in the range $1020 - 1098 \text{ cm}^{-1}$ corresponds to the internal vibrations of T-O-T where (T = Si or Al) tetrahedral structure [21]. Absorption between $443\text{-}465 \text{ cm}^{-1}$ is assigned to Si-O-Al stretching, where Al is in the octahedral coordination [20]. Vibration in the range $950\text{-}1250 \text{ cm}^{-1}$ is assigned to T-O stretching [22]. It can be seen that the FTIR spectrum of the zeolite prepared in the present work matches the typical absorption peaks of a commercial type [18]. The FTIR spectrum of the PA6 membrane is shown in Figure 4, in which the band at 3291 cm^{-1} is characteristic of N-H stretching [5], the 1637 cm^{-1} band is due to C=O stretching [5], the 1542 cm^{-1} band is related to vibration of N-H bending in amide [8], the narrow peaks between 1000 and 1200 cm^{-1} correspond to the C-O stretching vibrations in pure PA membrane [23] and the 685 cm^{-1} related to

vibration of NH swing [8]. Moreover, the spectrum shows two bands at 1415 cm^{-1} and 1477 cm^{-1} which are relate to the vibration of the CH_2 groups adjacent to NH and CO respectively [9]. It is also possible to identify bands in the range of $2915\text{--}2935\text{ cm}^{-1}$ due to CH molecular stretching [5],

Moreover, the 2850 cm^{-1} band is characteristic of CH_2 molecular stretching [9]. On the other hand, Figure 5 shows the FTIR spectrum of PA6/ZY membrane, where bands at 929 cm^{-1} and 957 cm^{-1} refer to the stretching of Si-O-T group[18]. The narrow peaks $420\text{--}500\text{ cm}^{-1}$ are due to T-O band in zeolite [18]. A slight increase in the intensity of PA membrane spectrum was observed when zeolite was added, which was consistent with the literature [10, 23] and due to weak interaction between functional groups of the zeolite and that of the polyamide [10]. The results of FTIR analysis reflect the nature of binding in the hybrid membranes PA6/ZY, by van der waals force or hydrogen bonds as refers literature [24]. Both membranes, PA6 and PA6/ZY, exhibit FTIR bands at 1200 cm^{-1} , 1415 cm^{-1} and 1477 cm^{-1} , related to α -crystalline phase vibrations. However, there is an absorption peak at 1169 cm^{-1} , related to amorphous phase's vibrations [9].

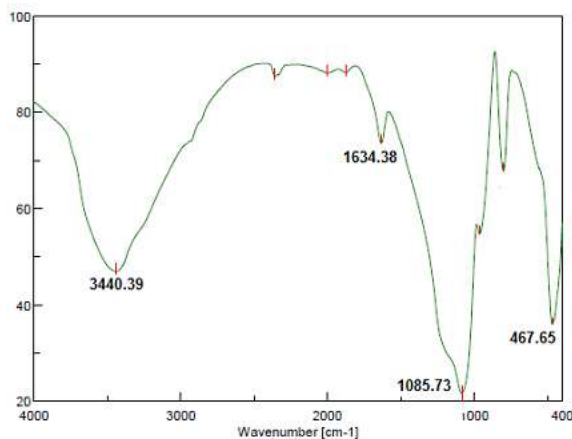


Fig. 3. FTIR Spectrum of laboratory prepared zeolite Y

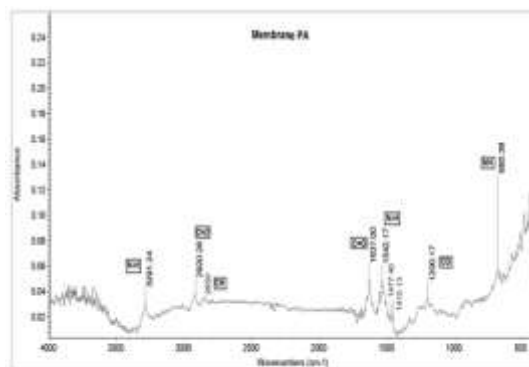


Fig. 4. FTIR Spectrum of pure PA6 membrane

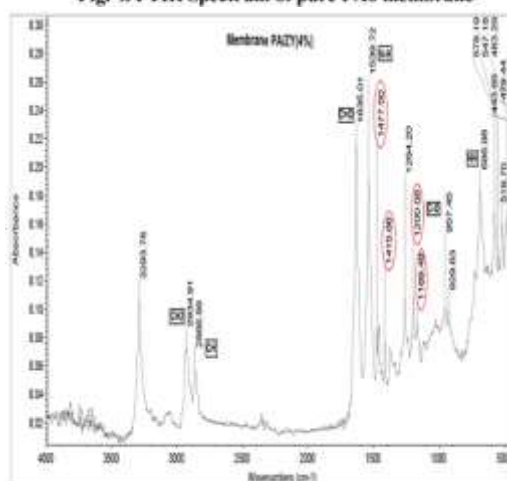


Fig. 5. FTIR Spectrum of PA6/ZY(4%) membrane

X-Ray Diffraction (XRD):

The diffractograms of laboratory prepared Zeolite Y is shown in Figure 6, where X-ray diffraction analysis was used to determine the degree of crystallinity. A 2θ range of 3° to 50° is usually adequate to cover the most important regions of the XRD pattern, and each peak represents at least one diffraction. Relative peak intensities are related to the extent of sample crystallization, and are determined by the type and position of all atoms in the unit cell [21]. The width of peaks is related to the size of crystallite, i.e. they can give an indication of samples crystalline quality [21]. Peaks observed by prepared zeolite Y in Figure 6 are similar to peaks of standard Zeolite Y shown in Figure 7(JCPDS 48-0038). The major peaks of identification on XRD pattern were located on $2\theta = 23.6^\circ$, $2\theta = 26.9^\circ$, and $2\theta = 31.3^\circ$. The XRD pattern also shows a peak in the range of $2\theta = 20\text{--}35^\circ$, which refers to crystallinity's degree [21,25], confirming the crystallization of prepared zeolite Y. The diffractograms of the membranes PA6 and (PA6/ZY) are shown in Figure 8. It is noticed that the

characteristic peaks of the zeolite Y disappears when it is incorporated to the polymeric matrix, indicating that a nanocomposite with exfoliated structure or partially exfoliated was obtained as shown in Figure 9. This result is consistent with others [6,7,9], where bentonite and montmorillonite were added to PA6 membranes. Peaks in the range of 17-26° in Figure 8 correspond to reflections related to the crystalline planes (200) and (002) of the α phase of polyamide-6, they were also observed in literatures [6,9,26]. There are also peaks in $2\theta=30^\circ$ and $2\theta=45^\circ$ referring to transmission intensity of the XRD [26]. Thus, it can be observed that crystallinity of membranes with inorganic filler is different from that of PA6, except the peak in $2\theta=45^\circ$ which increased in intensity. This behavior is due to hybrid membrane, which not only allows wide morphology variety but also influences the crystallinity of the polyamide.

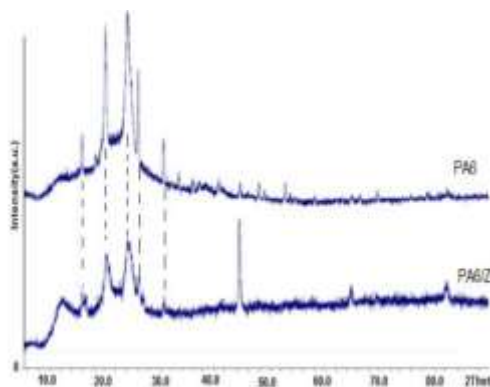


Fig. 8. XRD pattern of PA6 and PA6/ZY

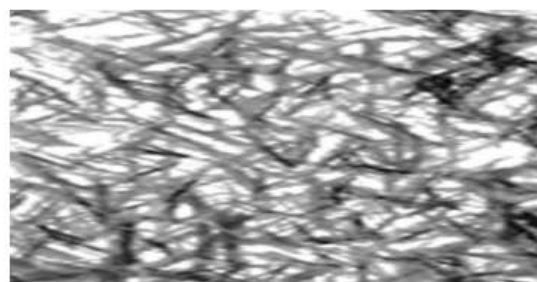


Fig.9 .Exfoliated (nanocomposite)

Scanning Electron Microscope (SEM):

The SEM images of prepared zeolite Y particles, shown in Figures 10 and 11 with scale bars of 500nm and 5 μ m, respectively, confirm the crystalline nature of the obtained zeolite. Zeolite crystals appear in the form of heterogeneous crystalline structures with cube and rectangular shapes. The cubic shape dominates by different diameters ranging from 100 to 270 nm. It is worth noting that the size of crystals was smaller than that of crystals obtained by Karami *et al* [13], due to the higher temperature (120° C) used during preparing zeolite.

Some particles apparently were connected to other particles, which was caused by long reaction associated with heating, as the mechanism of zeolitization is closely related to this effect [21]. Our results were in good agreement with that reported in literatures [13,20,21] and with X ray diffraction analysis.

The SEM image of PA membrane (Figure 12) shows a smooth surface with low gaps and low porosity. With zeolite in the membrane of PA/1% ZY and PA/4% ZY shown in Figures 13 and 14, the structure became more crystalline due to the presence of the crystalline zeolite. It was noticed that the gaps became more uniform in distribution, and increasing in number with increasing zeolite content in membrane. Nevertheless, Figure 13 shows that the amount of zeolite load in membrane (PA/1% ZY)

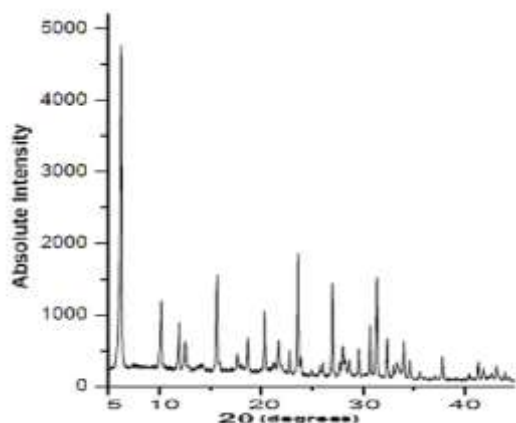


Fig. 6. XRD pattern of laboratory prepared Zeolite

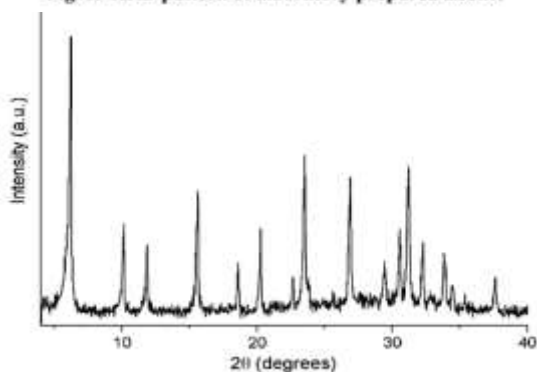


Fig. 7. XRD patterns of standard zeolite Y [18,25]

was insufficient to cover the entire surface. It also revealed that there were areas where the zeolite was agglomerated and areas with limited porosity. Figure 14 shows that, the amount of zeolite in the membrane was sufficient to be distributed over the entire surface, increasing roughness and porosity. Figure 15 shows the obtained PA/4% ZY membrane.

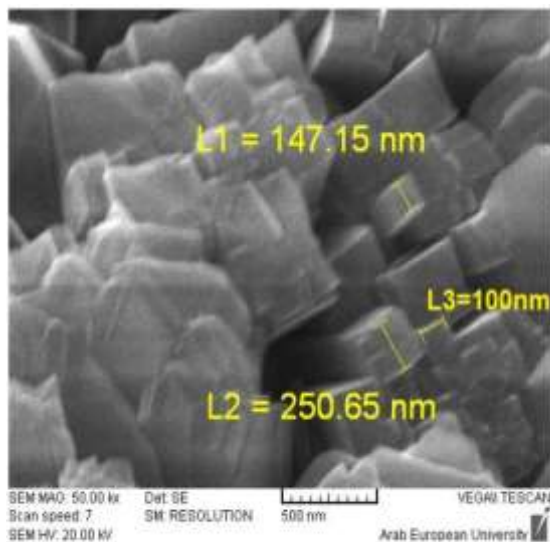


Fig. 10. SEM image of prepared zeolite Y particle at 500 nm spatial resolution

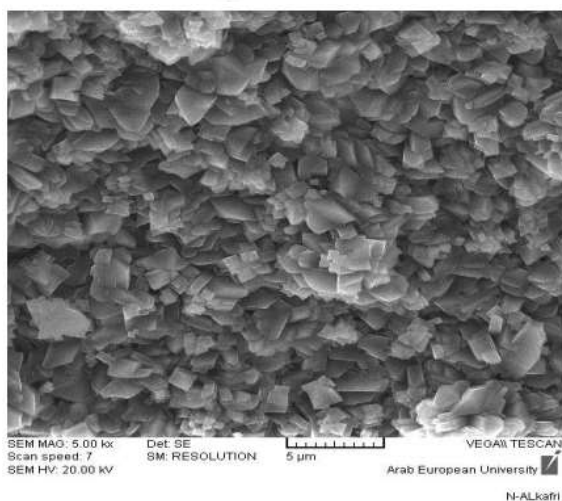


Fig. 11. SEM image of prepared zeolite Y particle at 5 μm spatial resolution

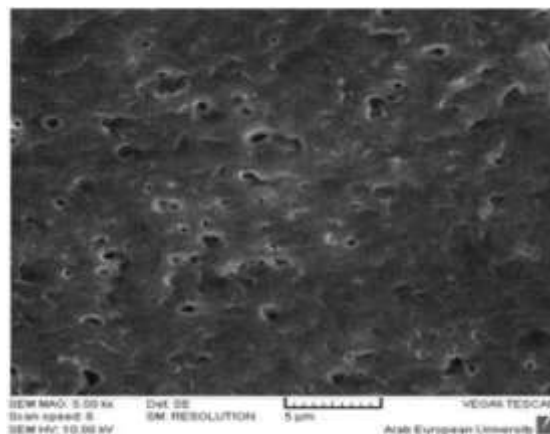


Fig. 12. SEM image of PA6 membrane particle at 5 μm spatial resolution

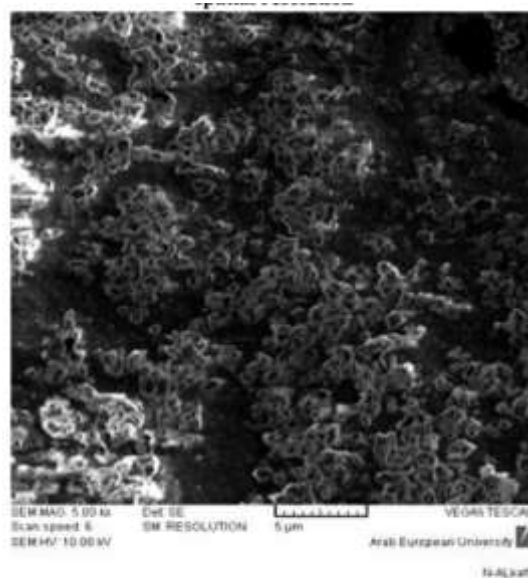


Fig. 13. SEM image of PA6 /1% ZY membrane particle at 5 μm spatial resolution

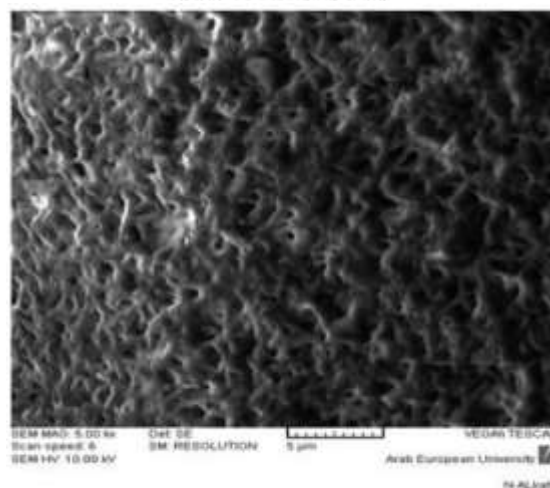


Fig. 14. SEM image of PA6 /4% ZY membrane particle at 5 μm spatial resolution



Fig.15. Image of PA6/4%ZY prepared membrane

Membrane porosity and pore size

Figure 16 shows the dependence of the porosity of the prepared membranes upon ZY loading, and Figure 17 shows their bubble point pressure and bubble point pore diameter.

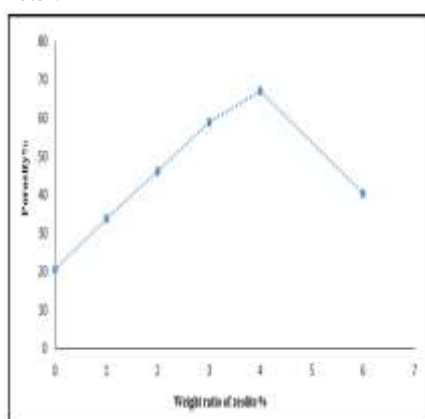


Fig. 16. Porosity of the membranes

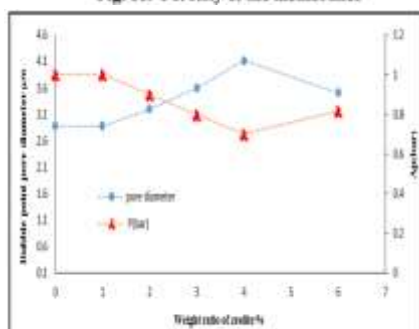


Fig. 17. Bubble point of pressure difference and bubble point pore diameter

It is clearly observed that the addition of zeolite increased porosity and bubble point pore diameter while decreased bubble point pressure of the membranes as results of SEM analyzes shows, section (3.4). These effects can be attributed to weak interface between micro-pores PA6 and zeolite due to poor compatibility between this inorganic particles and polymer, as FTIR analyzes proves, section (3.2). Whereas, when the content of zeolite exceeded 4%

the porosity and bubble pore diameter declined. This may be attributed to the excessive content of zeolite, which plugged some micro-pores and reduced penetration properties of the membrane. A similar phenomenon was found by hui Jiang *et al* [8] when adding SiO₂ to polyamide in concentrations of 5, 10 and 15%, where their results showed that the concentration of 10% yielded the best results in porosity and bubble point pore diameter.

3.6. Tensile strength and Strain:
The presence of nanoparticles within the membrane was supposed to improve the mechanical properties of the membrane, which depends on the amount of compatibility between the organic material (polymer) and the inorganic (zeolite) added to membrane. The improvement may be weak and limited owing to the difficulties associated with the intercalation of nonpolar chains inside the polar silicate interlayers [27].

The addition of zeolite decreased tensile strength and strain according to linear relationship as shown in Figure 18. This was attributed to clusters nanoparticles inside the membrane caused by the non-dispersion of enough zeolite granules inside the membrane. These results could be reflected on the crystallization behavior of the membrane, hence its properties, e.g. increasing the density of nanozeolite reduces the degree of crystallization [27], as shown in XRD study, section(3.3). In addition, the interaction of functional groups of PA6 with the zeolite surface were not strong enough to appear in the FTIR study, section (3.2), This referred to the limited amount of compatibility between PA6 and prepared zeolite. This indicated that the surface hardness increase with increasing the Zeolite content in the membranes.

Thus, the integration of zeolite into the PA6 matrix changes the surface characteristics of the composite materials significantly.

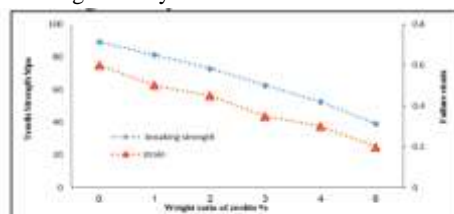


Fig. 19. Tensile strength, and Strain of prepared membranes

Conclusions

The zeolite Y has been successfully prepared using Sol-gel method under the influence of self-pressure at 120°C. XRD and SEM showed that the obtained zeolite Y nanocrystals were highly crystalline and

appeared in the cubic shape with different diameters ranging from 100 to 270 nm. The zeolite Y nanoparticles were embedded into the polyamide layer via interfacial polymerization with formed hybrid membranes (PA6/ zeolite Y). The hybrid membranes presented crystalline phases α . SEM also showed increasing the number of gaps in hybrid membranes with increasing of ZY content in the membrane. The optimum zeolite loading was determined to be 4% from polymer blend. Addition of zeolite to membranes increased its porosity, bubble point pore diameter, but its tensile strength and Failure strain decreased linearly. The presence of Zeolite nanoparticles changed the structure of the polyamide membrane by forming nano-gaps at the organic interfaces, which can reduced the crosslinking density of the polyamide layer. These obtained results show that membranes can be used effectively in water **filtration** subsequently.

Acknowledgment:

The authors would like to thank Damascus University and Atomic Energy Commission of Syria that have made this work possible.

References:

- [1] Baker R.W., Membrane Technology and Applications, Third Edition, Newark, California, 2nd Ed. Hoboken: John Wiley & Sons ,p14 (2012).
- [2] Kaushik N., Membrane Separation Processes, Second Edition, PHI Learning Private Limited, Delhi-110092, p.17(2017).
- [3] Tsung Y. T., Wei-Hsuan L., Yen-Yu L., YuChuan H., Umasankar R., Yue-Tang L., Ming-Jou O., Permeability property of Nylon 6 nanocomposite membranes with various clay minerals, *Desalination*, 233 ,183–190(2008).
- [4] El-Gendi A., Deratani A., Ahmed S.A., Ali S.S., Development of polyamide-6/chitosan membranes for desalination, *Egyptian Journal of Petroleum*, 23, 169-173(2014).
- [5] Hamid F., Akhbar S., Halim K.H. Ku., Mechanical and Thermal Properties of Polyamide 6/HDPE-g-MAH/High Density Polyethylene, *Procedia Engineering*, 68, 418 – 424(2013).
- [6] Ferreira R.S.B., Pereira C.H., Santos Filho E.A., Damião Leite A.M., Araújo E.M., Lucena Lira H.L., Coagulation Bath in The Production of Membranes of Nanocomposites Polyamide 6/Clay, *Mat. Res.* 20,117-125 (2017).
- [7] Medeirosa K.M., Araújo E.M., Lira H.L., Lima D.F., Lima C.A.P., Hybrid Membranes of Polyamide Applied in Treatment of Waste Water, *Mat. Res.* 20 (2), 308-316 (2017).
- [8] hui Jiang Z., Fa Xiao C., Wang X ., Yu Hu X., Structure And Performance Of Polyamide-6 Membranes Prepared By Thermally Induced Phase Separation, *Chinese Journal of Polymer Science* ,28(5), 721 -729 (2010).
- [9] Maia L.F., Leite A. M. D., Araújo E. M., Lira H. L., da Paz R. A., Spectroscopic And Diffraction Characteristics Of Membranes And Polyamide 6 /Regional Bentonite Clay Nanocomposites, *Materials Science Forum* ,775-776 , 168-172(2014).
- [10] Dong H., Zhao L., Zhang L., Chen H., Gao C., Winston Ho W.S., High-flux reverse osmosis membranes incorporated with NaY zeolite nanoparticles for brackish water desalination, *Journal of Membrane Science* , 476, 373-383(2015).
- [11] Yuxi Y., Rui M., Shaole y., Jiyu F., Preparation of multi-layer nylon-6 nanofibrous membranes by electrospinning and hot pressing methods for dye filtration, *RSC Adv*, 8, 12173–12178 (2018).
- [12] Yalcinkaya F., Yalcinkaya B., Hruza J., Electrospun Polyamide-6 Nanofiber Hybrid Membranes for Wastewater Treatment, *Fibers and Polymers* , 20(1), 93-99 (2019).
- [13] Karami. D and Rohani S., A Novel Approach for the Synthesis of Zeolite Y, *Ind. Eng. Chem. Res.* 48, 4837–4843(2009).
- [14] AL-Sayed M., Deri F., Preparation of Polyamide Membranes and Studies Their Chemical, Physical and Mechanical Properties and Its Application, *International Journal of ChemTech Research*, 5, 3098-3106(2014).
- [15] Cuperus F.P and Smolders C.A., Characterization of UF Membranes, Membrane Characteristics and Characterization Techniques, *Advances in Colloid and Interface Science*, 34, 135- 173(1991).
- [16] Shigidi I. M. T. A., The use of bubble point test in membrane characterization, *American Journal of Science and Technology*, 1(4), 140-144(2014).
- [17] Milisavljević J, Petrović E, Ćirić I, Mančić M, Marković D , Đorđević M, Tensile Testing For

- Different Types Of Polymers, Danubia-Adria Symposium, University of Belgrade, Serbia, 266-267(2012).
- [18] Nizam A.M., Surfactant Modified Zeolite Y As A Sorbent For Some Chromium And Arsenic Species In Water, A thesis submitted in fulfillment of the requirements for the award of the degree of Master of Science (Chemistry), Universiti Teknologi Malaysia, P.22 (2007).
- [19] Stamires D., Properties Of The Zeolite, Faujasite, Substitutional Series: A Review With New Data, *Clays and Clay Minerals*, 21, 379-389(1973).
- [20] Ahmedzeki N., Yilmaz S., Al-Tabbakh B., Synthesis and Characterization of Nanocrystalline Zeolite Y, *Al-Khwarizmi Engineering Journal*, 12(1), 79 – 89 (2016).
- [21] Matti A.H., Surchi K.M., Comparison the Properties of Zeolite Nay Synthesized by Different Procedures, *International Journal of Innovative Research in Science, Engineering and Technology*, 3(6), 13334- 13339(2014).
- [22] Deepesh B., Radha T., Purnima K. S., Yogesh G., Pankaj S., Hydrothermal Synthesis and Characterization of Zeolite: Effect of Crystallization Temperature, *Res. J. Chem. Sci.*, 3(9), 1-4 (2013).
- [23] Kong C., Shintani T., Tsuru T., Pre-seeding assisted synthesis of high performance polyamide zeolite nanocomposite membrane for water purification, Supplementary Material (ESI) for *New Journal of Chemistry*, 34, 2101 - 2104(2010).
- [24] Souza V. C., Quadri M. G. N., Organic Inorganic Hybrid Membranes In Separation Processes: A 10-Year Review, *Brazilian Journal of Chemical Engineering*, 30 (4), 683-700 (2013).
- [25] Zaidi S.S.A., A Step towards Continuous Production of NaY Zeolite in Amorphous Silica Particles using a Dry Process, A thesis submitted in partial fulfillment of the requirement for the degree of Doctor of Philosophy, Department of Chemical and Biochemical Engineering, The University of Western, Ontario London, Ontario, Canada, P86 (2010).
- [26] Shanak H., Ehses K.H., Gotz E., Leibenguth P., Pelster R., X-ray diffraction investigations of polyamide 6 films: orientation and structural changes upon uni- and biaxial drawing, *J Mater Sci*, 44, 655–663 (2009).
- [27] Mittal V., Polymer Layered Silicate Nanocomposites: A Review, *Materials*, 2, 992-1057(2009).
- تحضير وتوصيف أغشية بولي أميد ٦ زيوليت Y ودراسة خصائصها الفيزيائية والميكانيكية.
علا عدنان حميض وإيمان مصطفى البكري.
قسم الكيمياء – كلية العلوم – جامعة دمشق – سوريا.
- الملخص:**
تحضر الزيوليت Y بالطريقة الهيدروحرارية، ثم استُخدم في تحضير أغشية هجينة من بولي أميد 6 (PA6) والزيوليت Y. وصفت الأغشية الهجينة والزيوليت المحضر بانعراج أشعة (XRD) X، ومطيافية الأشعة تحت الحمراء (FTIR)، وماسح المجهر الإلكتروني (SEM) درست خواص الأغشية الفيزيائية (حجم المسام والمسامية) والميكانيكية (قوة الكسر والانفعال).
أظهرت النتائج أن للزيوليت بنية بلورية محددة، يتراوح حجم الحبيبات فيها من 100–270 nm (وأن الأغشية المهجنة ذات بنية مقشرة. تظهر دراسة طيف FTIR أغشية ZY/PA6 وجود زيادة طفيفة في شدة جميع العصابات بالمقارنة مع طيف غشاء PA6 بسبب قوى الارتباط الضعيفة في الأغشية المحضرة. تظهر نتائج المورفولوجيا أن غشاء PA ذو سطح أملس وفيه عدد قليل من الفجوات وبإضافة الزيوليت أصبح سطح الغشاء خشن وفيه عدد أكبر من الفجوات. وأن 4% وزناً تمثل أفضل تغطية للزيوليت في الأغشية. كما تُظهر النتائج أن مورفولوجيا الأغشية تتغير تبعاً لمحتوى الزيوليت فيها. أشارت الدراسة الريولوجية للأغشية أن إضافة الزيوليت إلى الأغشية يخفض خطياً من قوة الكسر والانفعالية في حين أن المسامية والقطر المكافئ للمسام